Astron. & Astrophys. 48, 63–73 (1976)

Optical and Radio Observations of the Galactic H II Region S 206 (NGC 1491)*

L. Deharveng
Observatoire de Marseille

F. P. Israel
Sterrewacht, Leiden

M. Maucherat
Laboratoire d'Astronomie Spatiale du CNRS, Marseille

Summary. The galactic emission nebula S 206 has been observed at 1415 MHz and 4995 MHz with the Westerbork Synthesis Radio Telescope. Interferograms in Hα, monochromatic photographs in Hβ, [O III], Hα and [N II], and high dispersion spectra near Hα were obtained at the Haute Provence Observatory. The nebula has a mean velocity $V_{LSR} = -26.5$ km s^{-1}, and a complex velocity field; S 206 is a high excitation nebula which contains an ionization front in the south and west. The exciting O 5 star is outside the brightest part of the nebula. The nebula is photon-limited in the south and west but open (density-limited) in the east. It is uniformly reddened with $E(B-V) \simeq 1$ mag. The brightest structures are an elephant trunk pointing towards the exciting star and globules probably containing neutral dense material. S 206 is an evolved H II region. Its structure, velocity field, and physical characteristics are best explained by a model similar to that of Orion A by Zuckerman (1973), Balick *et al.* (1974), and to that of NGC 2024 by Grasdalen (1974).

Key words: aperture synthesis radio observations — optical observations — structure of H II regions

I. Introduction

The optical nebula S 206 (NGC 1491, $\alpha_{1950} = 3^h59^m$, $\delta_{1950} = 51°11'$) is located in the Perseus arm (Georgelin, 1975). On the red print of the Palomar Sky Survey S 206 appears as an extended nebula (about 20′ in diameter) with absorption patches. Weak diffuse emission extends to about one degree east of the nebula. The blue print shows a bright central core about 3′ in diameter.

Table 1 lists the available radio observations obtained mostly with single dish instruments. The object clearly has an optically thin thermal spectrum at high frequencies. The spectrum turns over at a frequency below 750 MHz, probably around 260 MHz. A detailed study

* Optical observations were made at the Observatoire de Haute Provence.

Table 1. S 206 – Previous Radio Observations

Authors' Designation	Frequency (MHz)	Half-Power Beam-Width (arc min)	Flux-Density (f.u.)	Reference
4 CP 51.11 A	178	—	13.4	Caswell (1956)
NRAO 156	750	20	23.6±2.5	Pauliny-Toth *et al.* (1966)
CTB 12	960	48	30	Wilson and Bolton (1960)
S 206	1400	10	25.6±4	Felli and Churchwell (1972)
NRAO 156	1400	10	25.7±1.4	Pauliny-Toth *et al.* (1966)
DA 123	1420	36	17.1	Galt and Kennedy (1968)
S 206	2695	4.8	26.4	Walmsley *et al.* (1975)
NGC 1491	4995	6.4	18 ±1.8	Gebel (1968)
S 206	4995	2.6	16.0	Walmsley *et al.* (1975)
S 206	10690	0.25	10.7	Felli *et al.* (1974)

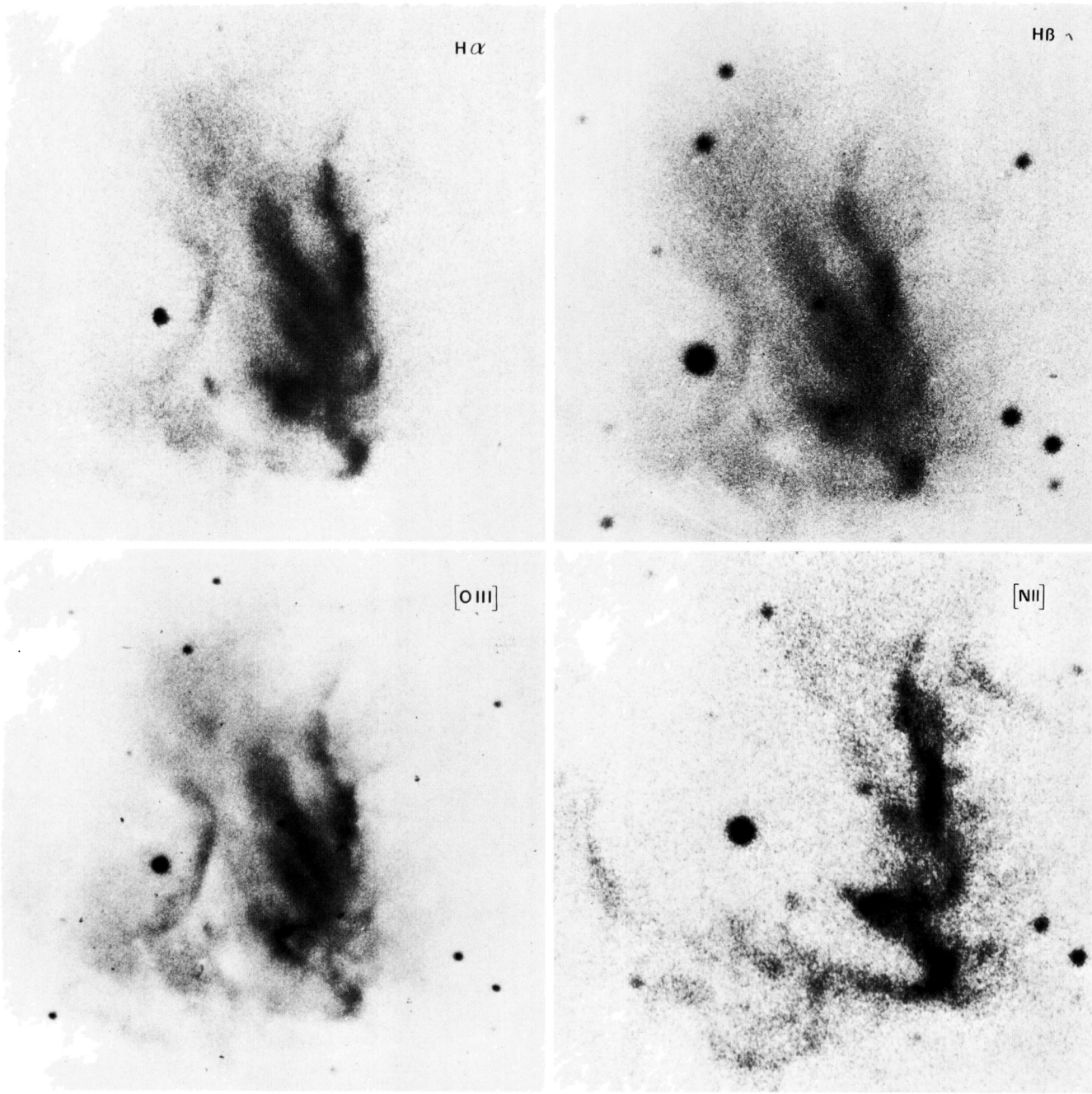

Fig. 1. Monochromatic photographs of S 206. The Hβ photograph was taken by M. C. Lortet

of the radio structure of S 206 was undertaken by Walmsley *et al.* (1975) who obtained radio maps at 2695 and 4995 MHz similar in appearance to the optical picture, albeit at much lower resolution (4'.8 and 2'.6 respectively.

Georgelin *et al.* (1973) identify BD + 50°886 as the exciting star. Crampton and Fisher (1974) class it as an O 5 V star.

Walmsley *et al.* (1975) searched the radio peak of S 206 and two off-positions east of the radio peak for H_2CO absorption, but did not detect anything. However, recent observations of CO emission (Blair *et al.*, 1975) establish the presence of two neutral clouds north-east and north-west of the radio peak. Unpublished observations of H I line emission with the 100 m telescope at Effelsberg indicate that S 206 coincides both in position and velocity with a neutral hydrogen maximum. Because of its size and structure, S 206 must be classified as an evolved H II region; also, no indication of young compact H II regions, or of recently formed stars has been found in this area: searches for OH masers (Fillit, quoted by Walmsley *et al.*, 1975), H_2O masers (Lo, 1974) and near infra-red emission (Bergeat and Sibille, private communication) have been fruitless.

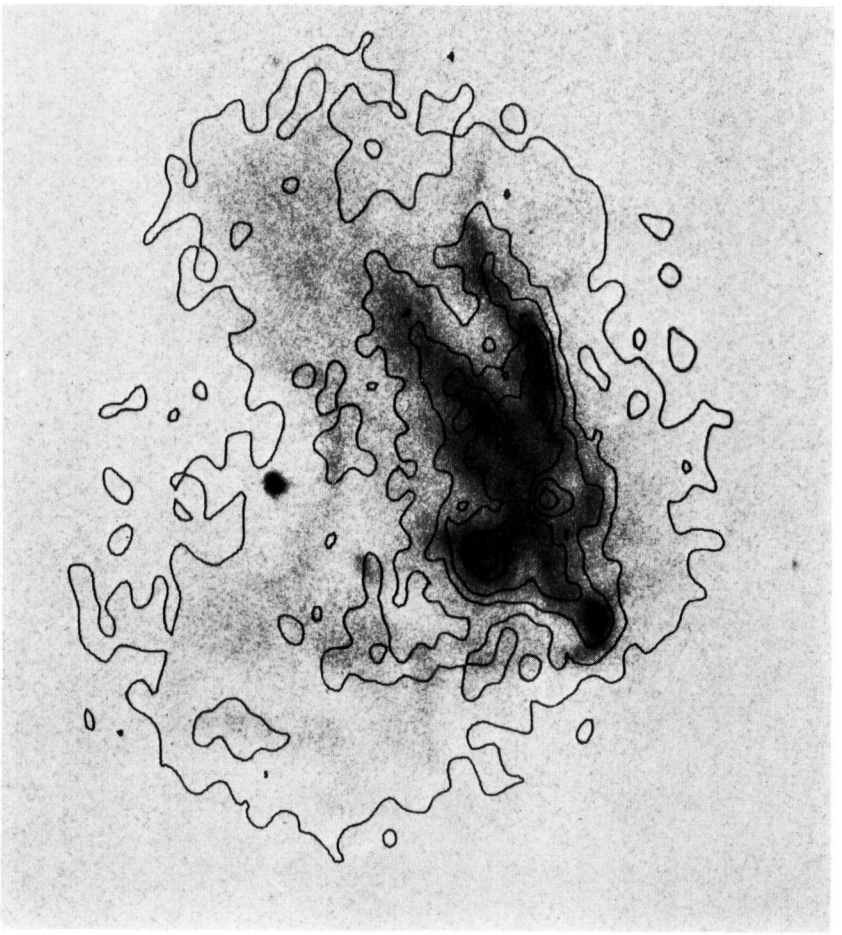

Fig. 1 bis. 6 cm radiomap of S 206 overlayed on the Hα photograph. The contour values are 6.25, 12.5, 18.75, 25, 37.50 and 50 m.f.u. per synthesized beam

Table 2. Monochromatic photographs

Line	Device used	Telescope	Aperture ratio	Exposure time	Emulsion
Hβ	Lallemand electronic camera	193 cm	*F*/5	30^m	Definix
[O III] λ 5007	Lallemand electronic camera	193 cm	*F*/5	45^m	Definix
Hα	Focal reducer	120 cm	*F*/3	1^h	Kodak 103 aE
[N II] λ 6584	Focal reducer and Image Tube	120 cm	*F*/2	30^m	baked Kodak IIaO

Because of its relatively high brightness at both radio and optical wavelengths, S 206 is an excellent object to study in detail. It is one of the few isolated nebulae excited by an O 5 star which is not a run-away star.

In this paper we present new optical observations in Section 2, new radio observations at high angular resolution in Section 3, while in Section 4 we discuss the kinematics, the optical and radio appearance, the excitation characteristics and the density distribution of S 206. In Section 5 a qualitative model is suggested.

II. Optical Observations

All the photographic, spectroscopic and interferometric observations were made at the Haute Provence Observatory. Figure 1 shows monochromatic photographs taken through narrow-band interference filters, ($\Delta\lambda \simeq 15$ A), in Hα, Hβ, [O III] λ 5007 and [N II] λ 6584.

Table 2 gives the observational conditions.

Five spectra were obtained with a nebular spectrograph, equipped with a RCA (C 33011 Type) image

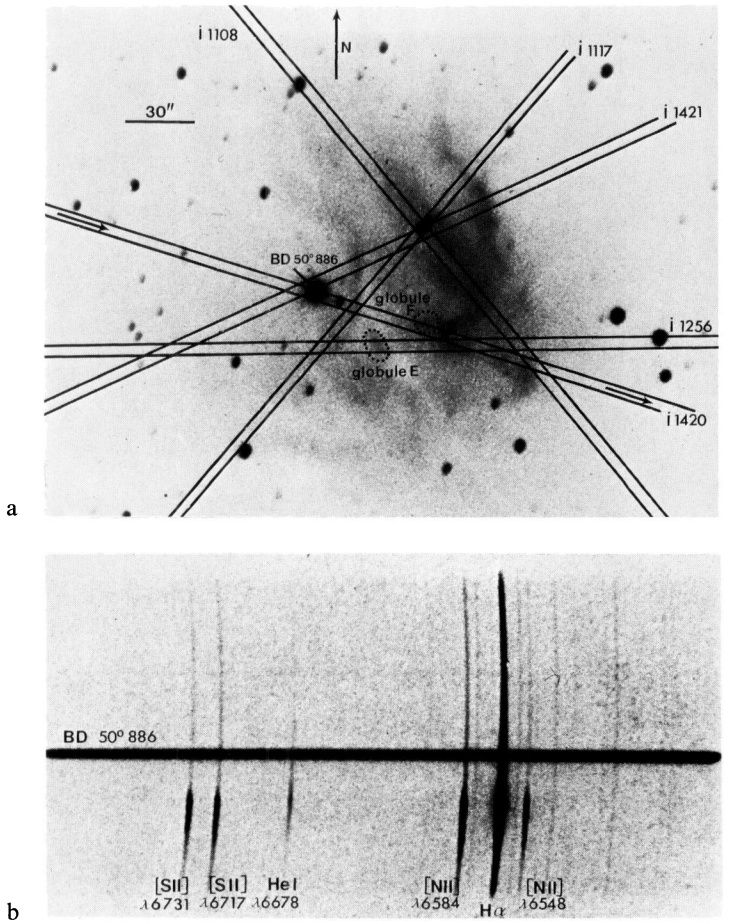

Fig. 2. a) Directions of the slit of the spectrograph. b) Spectrum I 1420

Table 3. S 206 – Radio Observations

Frequency (MHz)	1415	4995
Wavelength (cm)	21.2	6.0
HPBW Primary Beam (arc min)	37.6	12
HPBW Synthesized Beam (arc sec)	24.6 × 31.7	7.2 × 9.3
r.m.s. Noise (m.f.u. per beam)	1.2	1.3
Observing dates	71170 (HA −90/+15)	73241
	74230 (HA +15/+90)	
Interferometer spacings (m)	36–1404	36–1404
Increment (m)	72	72
Right ascension field-center	$04^h00^m00^s$	$03^h59^m24^s$
Declination field-center	+50°48′00″	+51°10′48″
Cleaned to level of (m.f.u. per beam)	11	10
Number of Components used in clean	153	139

tube, at the Cassegrain focus of the 193 cm telescope. Figure 2a indicates the slit orientation for these spectra, one of which is shown in Fig. 2b. The characteristics of the spectrograph (Pellet, 1975) are: entrance slit 420″ × 4.′6, plate scale 86″ mm^{-1}, dispersion 34 Å mm^{-1}. A spectral range of 350 Å includes Hα, [N II] λλ 6548–6584, He I λ 6678, [S II] λλ 6717–6731. The spectra were taken on baked Kodak IIaO plates. The photometric calibration procedure is discussed by Chopinet *et al.* (1974). We estimate the instrumental accuracy of intensity ratios to be about 10%.

The radial velocities for 93 points on the bright part of the nebula, were obtained from five recent interferograms in Hα, taken at the 120 cm telescope, at *F*/1. The exposure time varies from 30^m to 3^h. The interference order is 1360, which gives a dispersion of

Table 4. S 206 – Observed Radio Parameters

Component	Equatorial coordinates		Gal. coordinates		Flux-density		Angular diameter
	$\alpha_{1950.0}$	$\delta_{1950.0}$	l	b	S_{1415} (f.u.)	S_{4995} (f.u.)	θ (arc min)
Plateau 1[a])	$04^h01^m00^s$	$+51°05'00''$	150.83	−0.87	16.7	—	50
Plateau 2	03 59 40	51 10 00	150.62	−0.94	2.9	—	7.2 × 4.3
Core[b])	03 59 28	51 10 30	150.59	−0.96	6.0	5.8	4.3 × 3.6
Knot A	03 59 28.10	51 10 15.6	150.594	−0.959	–	0.080	0.18 × 0.19
Knot B	03 59 24.77	51 10 00.6	150.590	−0.967	–	0.020	0.08 × 0.11
Knot C	03 59 26.58	51 11 05.4	150.582	−0.951	–	0.025	0.08
K not D	03 59 26.22	51 10 13.2	150.591	−0.962	–	0.030	0.08 × 0.18

[a]) Based on comparison with 1400 MHz single dish observations in Table 1.
[b]) Includes contribution by knots A, B, C, D.

Table 5. Other sources in the field of S 206

Number	Equatorial coordinates		Corrected peak flux-density S_{1415} (f.u.)
	$\alpha_{(1950.0)}$	$\delta_{(1950.0)}$	
1	$03^h55^m45^s$	$+50°49'19''$	6.5
2	03 59 11	51 47 46	0.040
3	04 00 02	50 52 35	0.015
4	04 00 50	51 03 37	0.120
5	04 01 51	50 32 52	0.115
6	04 02 13	50 43 48	0.030

9 Å mm^{-1} at the first ring. The velocities are accurate to ± 4 km s^{-1}. Each velocity corresponds to a measured area of about $3'' \times 3''$.

III. Radio Observations

We used the Westerbork Synthesis Radio Telescope to observe S 206 at frequencies of 1415 and 4995 MHz. The telescope has been described in detail by Baars and Hooghoudt (1974). The λ 21 cm continuum receiver system was described by Casse and Muller (1974). Details relevant to the radio observations are given in Table 3.

We used the standard calibration and reduction procedures (Högbom and Brouw, 1974; Van Somersen Greve, 1974). The results of the radio observations are given in Table 4; physical parameters derived from Table 4, using a distance of 3.7 kpc, are given in Table 6. They were derived using a model of an homogeneous cylinder with a depth equal to its diameter and an electron temperature of 10^4 K (Mezger and Henderson, 1967).

Other sources detected in the field of S 206 at 1415 MHz are listed in Table 5. None of them has an optical counterpart on the Palomar Sky Survey prints. They are presumably all background radio galaxies. None of the sources is close enough to S 206 to be detected in the 4995 MHz map.

The following comments are in order:

1) in the original 1415 MHz observation, telescope B (spacings $36 + n \times 144$ m; $n = 1, 2, \ldots, 9$) failed from hour-angle $+15°$ to $+90°$ (end of observation). This hour-angle range was later reobserved.

2) the 1415 MHz field was not centered on S 206; as a consequence, the source is seriously weakened by the primary beam sensitivity decrease. A correction factor of 3.2 must be applied to the flux-densities of the components of S 206. The primary beam correction factor is already taken into account in the values given in Table 4, but not in the values given in the caption of Fig. 3.

Table 6. Physical parameters derived from the Radio Observations

Component	Linear diameter d(pc)	r.m.s. Electron density n_e(cm^{-3})	Emission measure EM(10^4 pc cm^{-6})	Mass $M(M_\odot)$	Excitation parameter u(pc cm^{-2})
Plateau 1	64	3.3	0.07	17500	83
Plateau 2	7.2	36.4	0.99	273	46
Core[a])	5.1	94.4	4.65	239	61
Knot A	0.24	1045	27.0	0.30	15
Knot B	0.12	1620	30.9	0.05	9
Knot C	0.10	2140	47.7	0.05	10
Knot D	0.15	1275	25.4	0.09	11
					$u_{total} = 97$

[a]) Includes contribution by knots A, B, C, D.

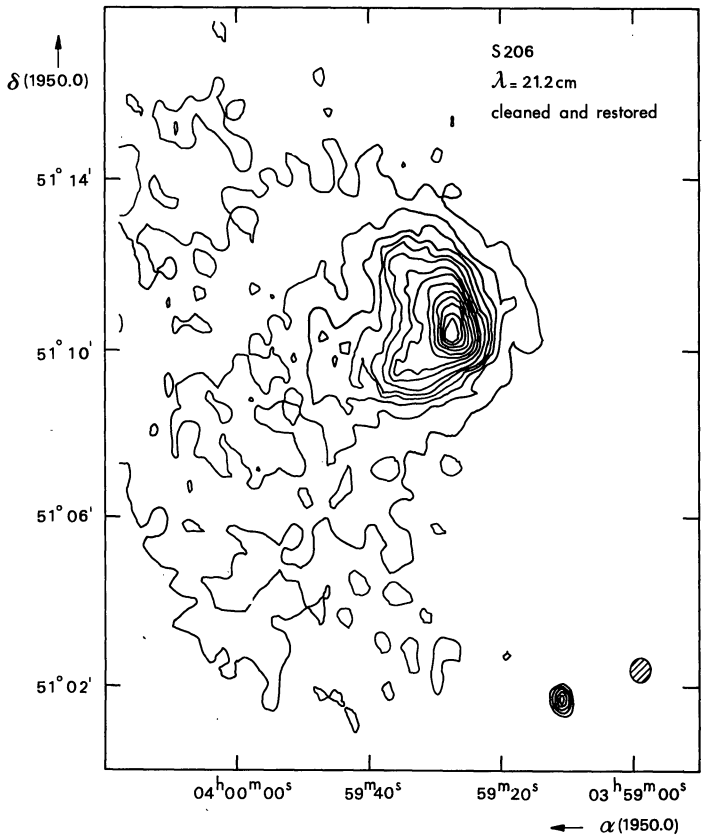

Fig. 3. Cleaned and restored radiomap of S 206 at 21 cm. The hatched area in the lower right hand corner indicates the size of the synthesized beam. The contour values are 5, 10, 15, 20, 25, 32.5, 42.5, 50, 62.5, 75, 87.5, 100, 112.5 and 125 m.f.u. per synthesized beam

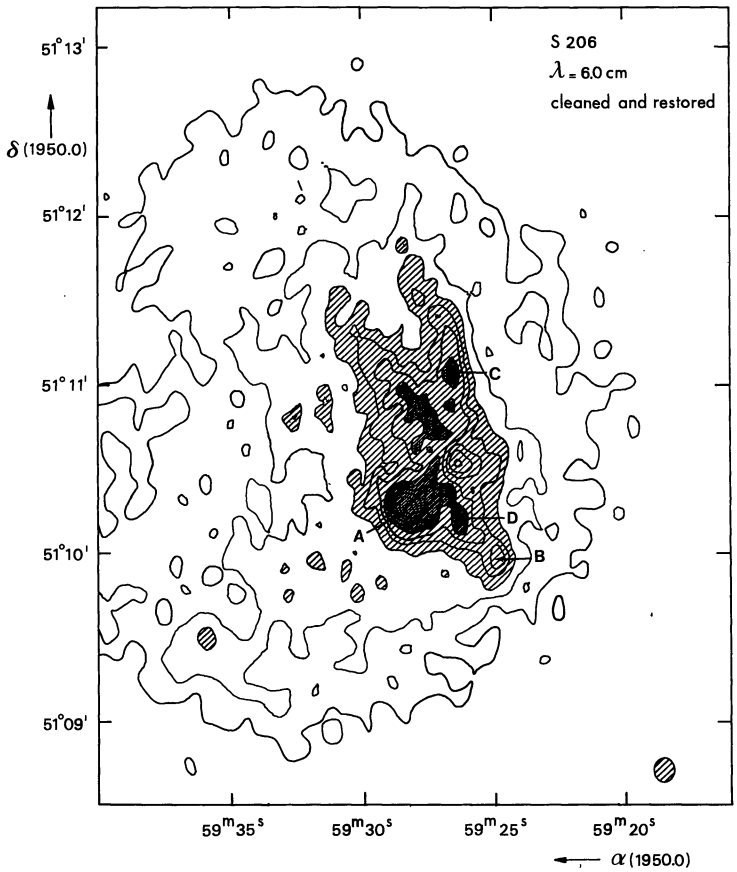

Fig. 4. Cleaned and restored radiomap of S 206 at 6 cm. The hatched area in the lower right hand corner indicates the size of the synthesized beam. The contour values are 5, 10, 15, 20, 25, 30, 35, 40, 45, 50 and 55 m.f.u. per synthesized beam

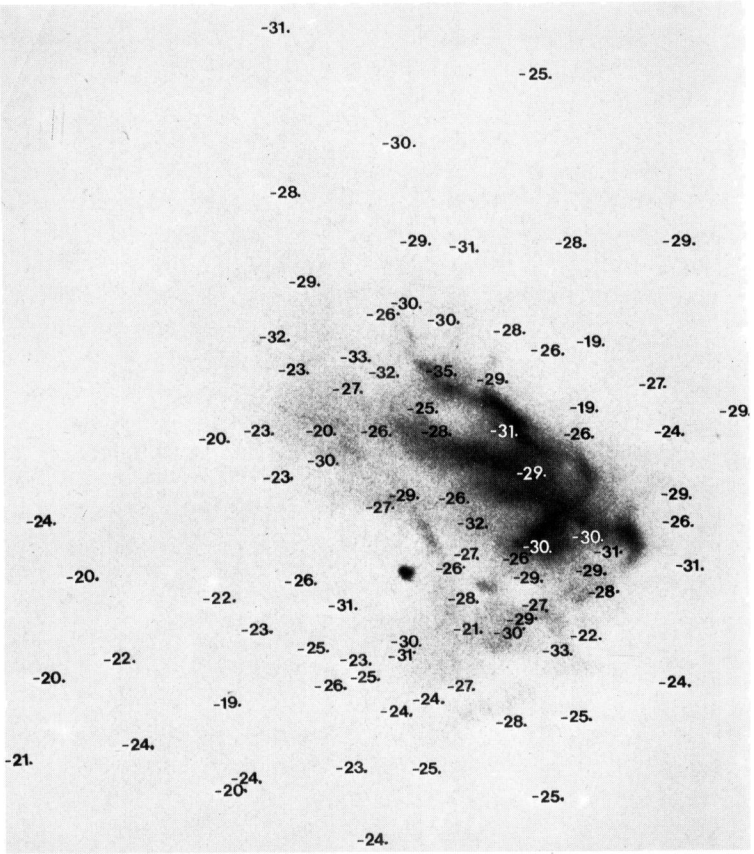

Fig. 5. V_{LSR} projected on the field of the nebula; the dots indicate the center of the measured area

3) the flux-density of S 206 was determined by planimetering the contourmaps; the values given are corrected for primary beam sensitivity decreases. At 1415 MHz the primary beam can be described roughly as a gaussian of the form $F_I(\%) = 100 \exp(-7.3R^2)$ where R is the distance to the beam center in degrees. At other wavelengths, the pattern scales approximately with wavelength. The estimated accuracy of the flux-densities determined in this way is 15%.

4) In order to separate actual source structure from instrumental effects as sidelobe interference, grating ring interference and zero level depression, the "*clean*" procedure (Högbom, 1974) was used in both radiomaps. The contourmaps presented in Figs. 3 and 4 are based on restored maps. They differ only in details from the original, uncleaned maps. We did not clean down to the actual zero level. For this reason a zero level depression is still present in the maps. Details of the clean procedure used are given in Table 3.

IV. Results

IV.1. Kinematics and Distance

Figure 5 shows the radial velocities projected on the field of the nebula. The velocity field is not clearly correlated with the optical structures. But there is a gradient of radial velocity of more than 10 km s^{-1}, from the south-east ($V_{LSR} \sim -20$ km s^{-1}) to the north-west ($V_{LSR} \sim -30$ km s^{-1}); also strong changes in velocity occur over small distances. An interpretation of this complex velocity field is given in Section 5. A mean radial velocity of -24.6 km s^{-1} is obtained from these new interferograms. The apex correction is -1.9 km s^{-1}, which gives $V_{LSR} = -26.5$ km s^{-1}. Table 7 lists the different determinations of V_{LSR}. There is a good agreement between the velocities deduced from radio recombination lines and Hα observations. The radial velocity of the nebula is also in good agreement with the radial velocity of -24.2 km s^{-1} given for the star BD+50°886 by Crampton and Fisher (1974).

A V_{LSR} of -26.5 km s^{-1} yields a kinematical distance of 2.3 kpc, according to the Schmidt model of galactic rotation. This distance is quite different from the photometric distance of 3.7 kpc for the star (Crampton and Fisher, 1974); the difference can be explained by systematic discrepancies to the Schmidt model of galactic rotation (Kerr, 1970; Georgelin, 1975). The distance of S 206 has been fully discussed by Walmsley *et al.* (1975); these authors, as well as Georgelin (1975) favour the photometric distance. In the following we assume a distance of 3.7 kpc.

Table 7. Determinations of V_{LSR}

Observed line	V_{LSR} km s^{-1}	Reference
Hα	-33.3 ± 3.9	Miller (1968)
Hα	-29.1	Georgelin (1969)
Hα	-24.0	Georgelin *et al.* (1973)
Hα	-26.5	This paper
H 109α	-26.3 ± 0.8	Walmsley *et al.* (1975)
He 109α	-25.3 ± 1.5	Walmsley *et al.* (1975)
H 137β	-26.1 ± 1.2	Walmsley *et al.* (1975)
CO emission	-22.2, -22.9	Blair *et al.* (1975)

IV.2. Optical and Radio Appearence

S 206 is very inhomogeneous both in optical and in radio emission.

Figure 1 shows that the exciting star BD+50°886 is located far away from the brightest area; the projected distance is about 1′, corresponding to a linear distance of 1.1 pc. The star is at the center of a "*half-ring*" nebulosity especially evident on the [O III] photograph; Hα photographs of long exposure time show no emission from the other half of the ring. The core of the nebula is composed, in the north, of two extensions of comparable intensities (except in [N II]), which join in the south. Diffuse and extended emission can be seen all around, both in the radio and the optical, even west of the steep edge of the nebula.

The north-western and southern extensions have the appearance of an ionization front: they have steep edges, show strong [N II] emission and an "*elephant trunk*" points very clearly to the exciting star.

The optical structure can be recognized easily in the radiomaps: all features seen on the Hα photograph are found on the 4995 MHz map (Fig. 1 bis). Moreover, the contrast ratios are approximately the same in both the Hα and the 4995 MHz pictures at all positions checked. Thus, the extinction varies little over the brightest part of the nebula, indicating the absence of large obscuring dust clouds.

IV.3. Excitation

S 206 is as a whole of high degree of excitation. The Hβ, [O III] and Hα photographs (Fig. 1) are very similar, although they are taken on different emulsions, with very different photometric properties; all the prominent structures in Hα and Hβ are apparent in [O III]. From low dispersion spectra (300 Å mm^{-1}), Chopinet *et al.* (1973) obtained for the brightest part of the nebula a high [O III]/Hβ ratio of 4.5. Also, the [N II]/Hα ratio remains low ($0.02\leqq$[N II]/Hα$\leqq0.25$, Fig. 6) over the whole nebula.

However, variations in the degree of excitation are observed over the field of the nebula, essentially from the [N II]/Hα ratio (Fig. 6); the degree of excitation is high around the star, in the half-ring nebulosity (strong [O III] emission, no [N II] emission) and in the north-eastern extension (this last region, which is of same Hβ intensity as the north-west extension, is absent on the [N II] photograph, Fig. 1); the excitation decreases steeply in the north-west and south extensions, and remains low west of the nebula. This is confirmed by the detection of [O I] λ 6300 emission in the north-west and south extensions (Chopinet, private communication). It probably indicates the presence of neutral dense material, as discussed by Capriotti *et al.* (1971) for the case of planetary nebulae. The north-west and south extensions very probably form an ionization front. On the contrary, because of its high degree of excitation, the half-ring nebulosity around the star cannot be an ionization front. It may be a shock-front in the ionized material.

From the radio observations we derive an excitation parameter for the whole nebula of $u=97$ pc cm^{-2}, which corresponds to an exciting star of spectral type O 5–O 6 (Panagia, 1973; Georgelin, 1975). Thus, BD+50°886 is very probably the only exciting star of S 206. Furthermore, it is possible that S 206 is only partially photon-limited as was already suggested by Walmsley *et al.* (1975). Probably some ionizing photons escape into the diffuse medium east of the H II region.

IV.4. Extinction

$E(B-V)_{neb}$ was recently determined from the Hα/Hβ ratio for a number of positions in S 206, by Chopinet (private communication)[1]). It indicates that the optical emission east of the bright core of S 206 – in the vicinity of the exciting star—is slightly less reddened ($E(B-V)\simeq$ 0.8 and 0.9) than the region west of the bright core ($E(B-V)\simeq1.1$ and 1.2). The bright core itself was not measured. The exciting star is slightly more reddened than the nebula: $E(B-V)_{star}=1.36$ ($A_V=4.05$ mag, Crampton and Fisher, 1974). These observations support the conclusion drawn in Section 4.2 that there are no dense dust cloud present in front of the nebula on a scale smaller than about 0.5 pc.

IV.5. Density Distribution

The electron density is derived from the intensity ratio of the two lines of the [S II] doublet λλ 6717–6731 (Saraph and Seaton, 1970, Table 3). Figure 7 shows the distribution of electron density in the bright part of the nebula. High electron densities are obtained in the "*elephant trunk*": about 6000 cm^{-3} is found at the head of this structure; high electron densities are also obtained in a small globule (Globule E, Fig. 2a) about 0.4 pc

[1]) Absolute Hα and Hβ fluxes were previously obtained by Gebel (1968) for the whole nebula (diaphragm: 1/4°); but he found a Hα/Hβ ratio = 1.52 which is obviously in error, as he already noted himself.

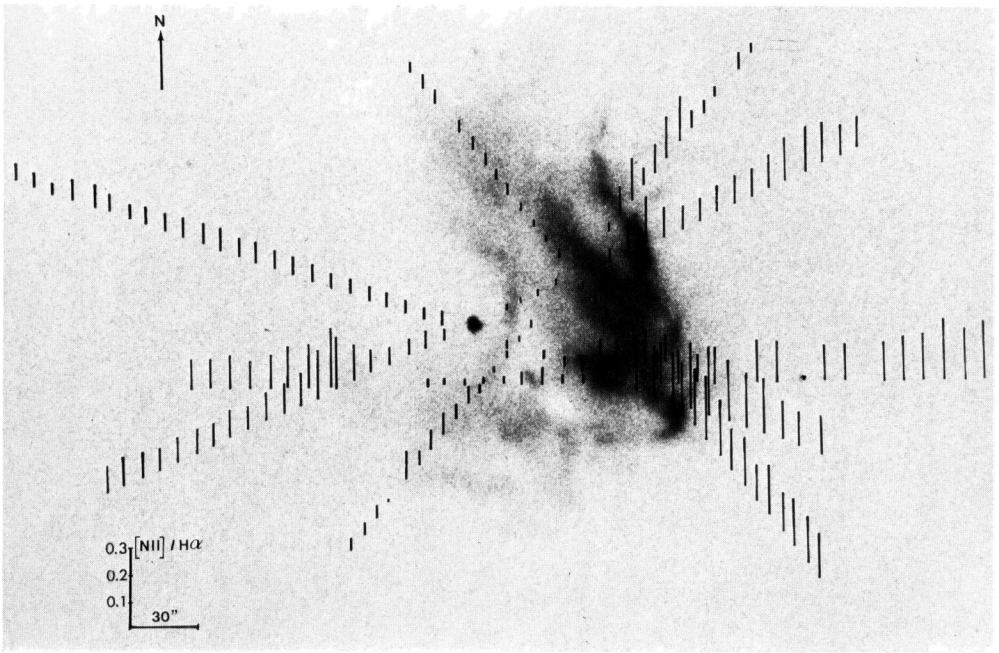

Fig. 6. Variations of the [N II]/Hα ratio over the field of the nebula; the foot of each segment indicates the point where the measure has been done; the size of the segments is proportional to the [N II]/Hα ratio

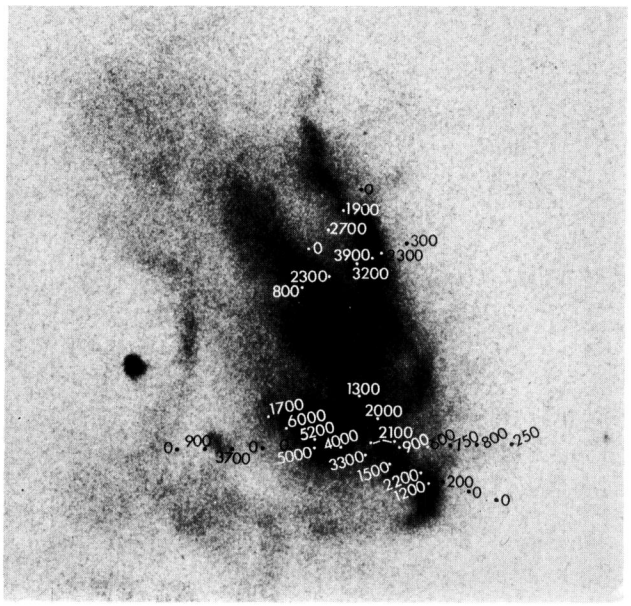

Fig. 7. Electron densities obtained from optical observations

Table 8. Electron densities in knots

Knot	Radio r.m.s. electron-density $\langle n_e^2 \rangle^{\frac{1}{2}}$	Mean optical electron-density	Clumping factor
A	1045	6000	33.
B	1620	2000	1.6
C	2140	3900	3.3
D	1275	1500	1.4

ahead of the "*elephant trunk*" ($n_e \sim 3700\,\mathrm{cm}^{-3}$) and in the north-west extension ($n_e \sim 3900\,\mathrm{cm}^{-3}$). The electron density decreases west of the nebula.

Electron densities obtained from optical observations are higher than the r.m.s. electron densities obtained from radio observations (Table 8). This indicates the presence of electron density gradients inside S 206. However, the clumping factor ($n^2_{\mathrm{opt}}/\langle n_e^2 \rangle$) for components B, C, D is only in the order 1.4–3.3, indicating that the electron density gradients are not very steep; the structures are essentially resolved in the 4995 MHz radiomap. Only for knot A (clumping factor 33), the present resolution is insufficient; this is also clear from the direct comparison of the optical photographs, notably the one in [O III], with the 4995 MHz radiomap.

Figure 8 shows the distribution of the intensities of Hα, [N II] and [S II], of the [N II]/Hα ratio and of the electron density, along the direction of the slit, going from east to west through the "*elephant trunk*". The electron density increases very steeply east of the "*elephant trunk*" (from 0 to 6000 cm^{-3} in 0.2 pc); such a steep increase of the electron density at the edges of this "*elephant trunk*" is also found in another spectrum. The peak electron density is 13″ (0.23 pc) east of the peak line intensity, in the direction of the exciting star.

Thus, we observe in globule E (Fig. 2a) a region where the electron density is high, and the radio emission low (Fig. 4). To explain both a high electron density and a

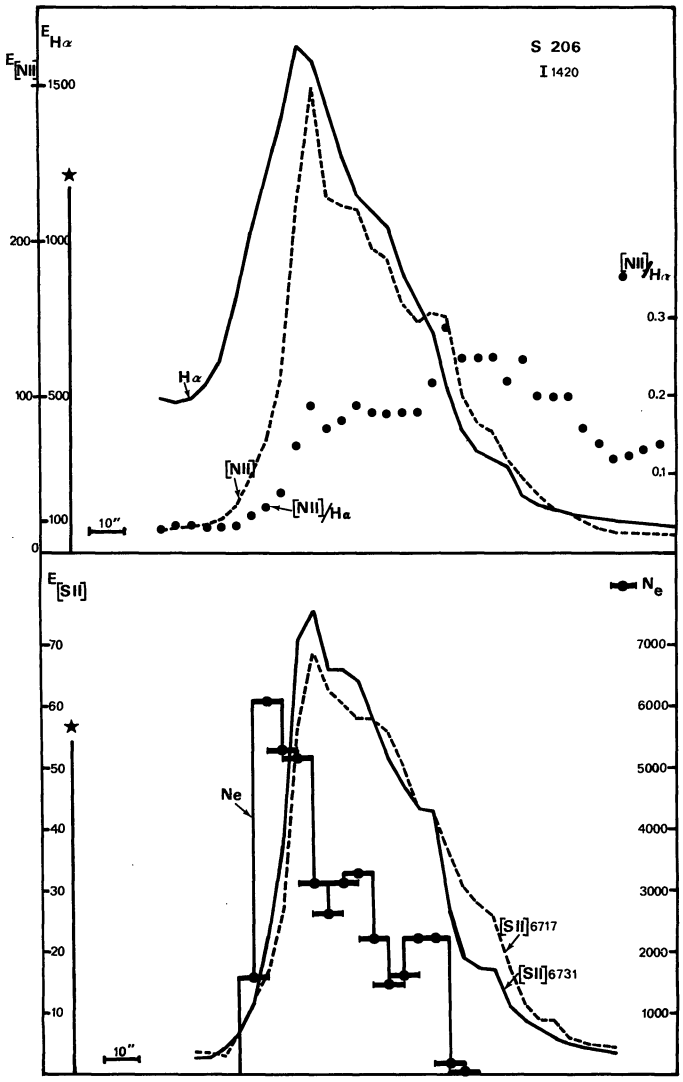

Fig. 8. *Top*: distribution of the Hα and [N II] intensities, and of the [N II]/Hα ratio (dots) along the direction of the slit for spectrum *I* 1420. *Bottom*: distribution of the [S II] intensities and of the derived electron density N_e (dots) along the direction of the slit. The bar on each dot represents the dimension of the region for which we have determined the electron density. The tracing from left to right is in the sense indicated by arrows on Fig. 2a. The scale of the abcissa is given by a bar at the bottom of the figure; the star is BD 50°886

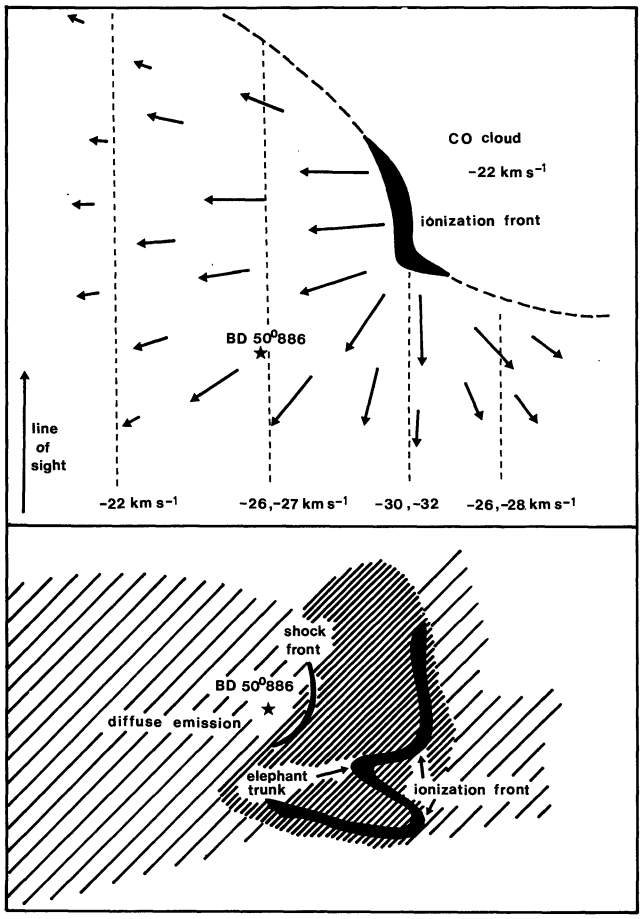

Fig. 9. Proposed model for S 206: *Top*: cross section of the nebula in a plane containing the observer and the exciting star, and perpendicular to the ionization front. The arrows represent the velocities of the streams of ionized gas. The numbers at the bottom are the velocities averaged along the line of sight. *Bottom*: schematic view of S 206 as seen from the Earth

small emission measure, we must assume that the length along the line of sight of the emiting region is small. That can be the case if globule E is the ionized region surrounding a neutral dense condensation. This hypothesis is confirmed by the detection of the [O I] λ 6300 emission from this globule (Chopinet, private communication). A high electron density of 6000 cm^{-3} is obtained at the edge of globule F (Figs. 2a and 7); in this region there is a lack of correlation between the distributions of electron density and line intensities (Fig. 8). This can also be explained by the presence of a neutral dense condensation along the line of sight. Globules E and F could represent the last stage of the evolution of an "*elephant trunk*" (Pottasch, 1965).

V. The Nature of S 206

S 206 emerges from the preceding as an evolved H II region. It contains no separate small scale compact component, and its most outstanding feature is an ionization front. The nebula appears to be open (mass-limited) to the east, while it is photon-limited to the west. CO emission (Blair *et al.*, 1975) is found north-east and north-west of S 206, while no H_2CO absorption (Walmsley *et al.*, 1975) is detected near the nebula. Comparable densities are required to excite these lines ($n_H \geqq 10^3$ cm^{-3}—of the same order as the electron densities deduced in this paper for the dense parts of S 206, near the ionization front). Thus, the non-detection of H_2CO is likely due to the fact that the neutral cloud lies alongside and behind S 206. We suggest the following model for S 206 (Fig. 9).

The exciting star BD 50°886 is at the present epoch outside the boundaries of the neutral cloud. It may have come into existence at the edge of the cloud. The star is ionizing the nearest part of the neutral cloud.

Advancing in a direction, roughly perpendicular to the line of sight, an ionization front is slowly eating its way into the dense neutral medium with a velocity in the order of 0.03 km s^{-1} (neutral gas with $T=100$ °K). From this front, ionized matter is streaming away with a velocity in the order of 10–15 km s^{-1}, this velocity decreasing as we move away from the front. Most of this gas is streaming away in a direction more or less perpendicular to the line of sight, so that the observed radial velocities do not differ strongly from the velocity of the neutral cloud ($V_{CO}=-22$ km s^{-1}). This model, which is similar to the model presented by Zuckerman (1973) and Balick *et al.* (1974), for the Orion Nebula (NGC 1976) and to the model presented by Grasdalen (1974) for Orion B (NGC 2024), explains in a consistent manner several observed phenomena.

1) The model explains the observed velocity gradient, in the sense that the diffuse emission east of the central star has a velocity comparable to that of the neutral cloud ($V_{LSR}=-22$ km s^{-1}), while the velocity is much more negative at the position of the ionization front. The observed radial velocity is smaller again for the diffuse emission west of the front (Fig. 9).

2) The idea of streams explains also the abrupt velocity changes in different parts of the nebula, and the filament structure of the nebula.

3) The observed density structure—high at or near the front—also supports the notion of gas expanding away from the ionization front. It should be noted that the idea of rotation is inconsistent with most of the observations presented here. Moreover, since the two neutral clouds have similar velocities (-22.2 km s^{-1}, -22.9 km s^{-1}, Blair *et al.*, 1975), the CO observations are hard to reconcile with any idea of rotation.

At present, the star does not appear to lose mass at a high rate, but the presence of a shock-front—the half ring nebulosity—reminiscent of the "Bubble Nebula" NGC 7635 in S 162 (cf. Icke, 1973) may indicate a stronger activity in the past. It is noteworthy that the shock-front is best defined in the direction of highest density, but also in the most probable direction of streaming. The absence of OH/H_2O maser emission and strong near infrared source indicates that no star formation is actively taking place in or near S 206.

Acknowledgements. It is a pleasure to thank H. J. Habing, J. Caplan, M. C. Lortet and G. Monnet for their critical reading of the manuscript.

We also want to thank J. Bergeat, G. N. Blair, M. Chopinet, E. Churchwell, Y. P. Georgelin and F. Sibille for making available to us the results of their observations prior to publication.

The Westerbork Synthesis Radio Telescope is operated by the Netherlands Foundation for Radio Astronomy which is financially supported by the Netherlands Organization for the Advancement of Pure Research (Z.W.O.).

References

Baars, J. W. M., Hooghoudt, B. G. 1974, *Astron. & Astrophys.* **31**, 323
Balick, B., Gammon, R. H., Hjellming, R. M. 1974, H II regions and the Galactic Centre, 8th ESLAB *Symposium*, Ed. A. F. M. Moorwood, ESRO SP-105
Blair, G. N., Peters, W. L., Van den Bout, P. A. 1975, *Astrophys. J.* **200**, L 161
Capriotti, E. R., Cromwell, R. H., Williams, R. E. 1971, *Astrophys. Letters* **7**, 241
Casse, J. L., Muller, C. A. 1974, *Astron. & Astrophys.* **31**, 333
Caswell, J. L. 1966, Thesis, University of Cambridge
Chopinet, M., Georgelin, Y. M., Lortet-Zuckermann, M. C. 1973, *Astron. & Astrophys.* **29**, 225
Chopinet, M., Deharveng, L., Lortet-Zuckermann, M. C. 1974, *Astron. & Astrophys.* **30**, 233
Crampton, D., Fisher, W. A. 1974, *Publ. Dominion Astrophys. Obs.* **14**, no 12
Felli, M., Churchwell, E. 1972, *Astron. Astrophys. Suppl.* **5**, 369
Felli, M., Tofani, G., D'Addario, L. R. 1974, *Astron. & Astrophys.* **31**, 431
Galt, J. A., Kennedy, J. E. D. 1968, *Astron. J.* **73**, 135
Gebel, W. L. 1968, *Astrophys. J.* **153**, 743
Georgelin, Y. P. 1969, Thesis, Université de Provence
Georgelin, Y. P., Georgelin, Y. M., Roux, S. 1973, *Astron. & Astrophys.* **25**, 337
Georgelin, Y. M. 1975, Thesis, Université de Provence
Grasdalen, G. L. 1974, *Astrophys. J.* **193**, 373
Högbom, J. A. 1974, *Astron. & Astrophys. Suppl.* **15**, 417
Högbom, J. A., Brouw, W. N. 1974, *Astron. & Astrophys.* **33**, 289
Icke, V. 1973, *Astron. & Astrophys.* **26**, 45
Kerr, F. J. 1970, IAU *Symp.* **38**, 95
Lo, K. Y. 1974, Thesis, Mass. Inst. Technology
Mezger, P. G., Henderson, A. P. 1967, *Astrophys. J.* **147**, 471
Miller, J. S. 1968, *Astrophys. J.* **151**, 473
Panagia, N. 1973, *Astron. J.* **78**, 929
Pauliny-Toth, I. I. K., Wade, C. M., Heeschen, D. S. 1966, *Astrophys. J. Suppl.* **13**, 65
Pellet, A. 1975, Thesis (in preparation)
Pottasch, S. R. 1965, *Vistas Astron.* **6**, 149
Saraph, E. H., Seaton, M. J. 1970, *Monthly Notices Roy. Astron. Soc.* **148**, 367
Van Someren Greve, H. W. 1974, *Astron. Astrophys. Suppl.* **15**, 343
Walmsley, C. M., Churchwell, E., Kazès, I., Le Squéren, A. M. 1975, *Astron. & Astrophys.* **41**, 121
Wilson, R. W., Bolton, J. G. 1960, *Publ. Astron. Soc. Pacific* **72**, 331
Zuckerman, B. 1973, *Astrophys. J.* **183**, 863

L. Deharveng
Observatoire de Marseille
2, place Le Verrier
F-13004 Marseille, France

F. Israel
Sterrewacht – Huygens Laboratorium
Wassenaarseweg 78
Leiden 2405, The Netherlands

M. Maucherat
Laboratoire d'Astronomie Spatiale
Traverse du Siphon
Les Trois Lucs
F-13012 Marseille, France